

IOWA STATE UNIVERSITY

Digital Repository

Biochemical Engineering Symposium Proceedings

Chemical and Biological Engineering

4-29-1972

Second Annual Kansas State–Nebraska Biochemical Engineering Symposium (April 29, 1972)

Peter J. Reilly

Iowa State University, reilly@iastate.edu

Follow this and additional works at: http://lib.dr.iastate.edu/bce_proceedings



Part of the [Biochemical and Biomolecular Engineering Commons](#)

Recommended Citation

Reilly, Peter J., "Second Annual Kansas State–Nebraska Biochemical Engineering Symposium (April 29, 1972)" (1972). *Biochemical Engineering Symposium Proceedings*. 2.

http://lib.dr.iastate.edu/bce_proceedings/2

This Book is brought to you for free and open access by the Chemical and Biological Engineering at Iowa State University Digital Repository. It has been accepted for inclusion in Biochemical Engineering Symposium Proceedings by an authorized administrator of Iowa State University Digital Repository. For more information, please contact digirep@iastate.edu.

SECOND ANNUAL
KANSAS STATE - NEBRASKA
BIOCHEMICAL ENGINEERING SYMPOSIUM

April 29, 1972

BIOCHEMICAL ENGINEERING SYMPOSIUM PROCEEDINGS

This booklet contains abstracts of papers presented at a biochemical engineering symposium conducted at the University of Nebraska-Lincoln on April 29, 1972. This was the second annual symposium on this subject, the first having been held at Kansas State University on June 4, 1971. It is expected that future symposia will alternate between the two campuses.

Those participating from Kansas State were Larry E. Erickson, I. C. Kao, Juan Lizcano, George Chu, J. S. Shastri, Thomas Kuo, P. N. Mishra, Kenneth Hsu, C. R. Lee, and S. H. Lin. Nebraska attendees were Peter J. Reilly, Shinji Goto, William J. Young, Chil-yuk Choi, Gregory C. Martin, Mark C. Young, Andrew Chan, Kenneth Jacobson, Bradford Jones, and Lincoln Yang.

Further information on the projects presented here can be obtained from Prof. Larry E. Erickson at Kansas State University or Prof. Peter J. Reilly at the University of Nebraska-Lincoln.

Peter J. Reilly
Editor

Biochemical Engineering Symposium
Avery Laboratory
University of Nebraska - Lincoln
April 29, 1972

- 10:00 - S. H. Lin, Kansas State University, "Enzyme Reaction in a Tubular Reactor with Laminar Flow"
- 10:30 - Gregory C. Martin, University of Nebraska, "Estimation of Parameters in Population Models for Schizosaccharomyces pombe from Chemostat Data"
- 11:00 - Jaiprakash S. Shastri and Prakash N. Mishra, Kansas State University, "Immobilized Enzymes: Analysis of Ultrafiltration Reactors"
- 11:30 - Mark D. Young, University of Nebraska, "Modelling Unsteady-State Two-Species Data Using Ramkrishna's Staling Model"
- 12:00 - Lunch
- 1:30 - G. C. Y. Chu, Kansas State University, "Optimization of Step Aeration Waste Treatment Systems Using EVOP"
- 2:00 - Shinji Goto, University of Nebraska, "Growth of the Blue-Green Alga Microcystis aeruginosa under Defined Conditions"
- 2:30 - Prakash N. Mishra and Thomas M. C. Kuo, Kansas State University, "Digital Computer Simulation of the Activated Sludge System: Effect of Primary Clarifier on System Performance"
- 3:00 - Mark D. Young, University of Nebraska, "Aerobic Fermentation of Paunch Liquor"
- 3:30 - 5:30 - Free Time
- 5:30 - Informal Dinner

ENZYME REACTION IN A TUBULAR REACTOR WITH LAMINAR FLOW

S. H. Lin
Department of Chemical Engineering
Kansas State University
Manhattan, Kansas 66502

INTRODUCTION

Enzymatic reactions have drawn considerable attention in recent years. Because of the vast opportunity they open up for innovation of chemical technology, they are of special interest to chemical engineers. Enzymatic reaction has many distinct advantages. At room temperature, enzymatic reaction rates may be many orders of magnitude higher than those of ordinary chemical reactions. Thus, enzymatic reactions do not need severe reaction conditions such as high pressure and high temperature which are often encountered in chemical catalytic processes. Furthermore, enzymes have an amazing specificity toward substrates. This fact makes enzymes ideal catalysts.

In a recent review article, Carbonell and Kostin (1) pointed out the importance of enzymatic technology in the near future. These authors presented a rather complete list of references on enzymatic kinetics and enzyme engineering. It is surprising to find that there is only a very meager literature available on enzymatic reactor design in comparison to the extensive literature of reactor design of other chemical processes. Generally speaking, enzymatic reaction is quite similar to other chemical reaction except for the reaction rate term. In enzymatic reaction, the reaction rate is represented by the well-known Michaelis-Menten equation. The general mathematical model of chemical reaction is readily applicable to enzymatic reaction. To the author's knowledge, there is only one recent paper by Kobayashi and Moo Young (2) dealing with enzymatic reaction in a packed-bed reactor. They considered enzymatic reaction under isothermal conditions.

There is no literature available on enzymatic reaction in a tubular reactor with laminar flow. This work is concerned with the behavior of a nonisothermal enzymatic reaction in a laminar flow tubular reactor. Mathematical formulation is modeled after that used in other chemical reaction processes. The effects of reaction heat generation and other kinetic parameters on the substrate conversion are examined. It is expected that this work may provide a better understanding of the enzymatic reaction behavior in a laminar flow reactor.

MATHEMATICAL MODEL

Consider a reactor through which the substrate passes at a velocity $u(r)$. Conservations of mass and energy give rise to

the following dimensionless differential equations:

$$(1-R^2) \frac{\partial C}{\partial X} = \frac{\partial^2 C}{\partial R^2} + \frac{1}{R} \frac{\partial C}{\partial R} - \frac{WC}{C+K} \exp\left(-\frac{\theta}{\theta}\right) \quad (1a)$$

$$(1-R^2) \frac{\partial \theta}{\partial X} = \frac{\partial^2 \theta}{\partial R^2} + \frac{1}{R} \frac{\partial \theta}{\partial R} + \frac{WGC}{C+K} \exp\left(-\frac{\theta}{\theta}\right) \quad (1b)$$

subject to

$$X = 0 ; \quad C = 1 \quad , \quad \theta = 1 \quad (2a)$$

$$R = 0 ; \quad \frac{\partial C}{\partial R} = 0 \quad , \quad \frac{\partial \theta}{\partial R} = 0 \quad (2b)$$

$$R = 1 ; \quad \frac{\partial C}{\partial R} = 0 \quad , \quad \frac{\partial \theta}{\partial R} = B(1-\theta) \quad (2c)$$

Detailed derivations of the above equations are presented elsewhere (3).

Eqs. (1a) and (1b) are coupled together through the reaction term. Hence, it is unlikely that they are tractable to analytical solutions. For the present work, an iterative numerical method of Crank-Nicolson scheme is employed to overcome the mathematical difficulty. Detailed solution method and the specification of the parameters also are presented in Reference 3.

RESULTS

A typical preliminary numerical result is shown in the accompanying figure. The following conclusions can be drawn from the results obtained:

- (1). Exothermic reaction generally favors the substrate conversion provided that the mixture temperature does not exceed the enzyme deactivation temperature.
- (2). The effect of temperature on substrate conversion is rather pronounced at low K (Michaelis-Menten constant divided by inlet substrate concentration), however, as K increases, the effect of temperature is significantly reduced and at $K \geq 4$, the isothermal solution gives good approximate prediction of the enzymatic reaction behavior.

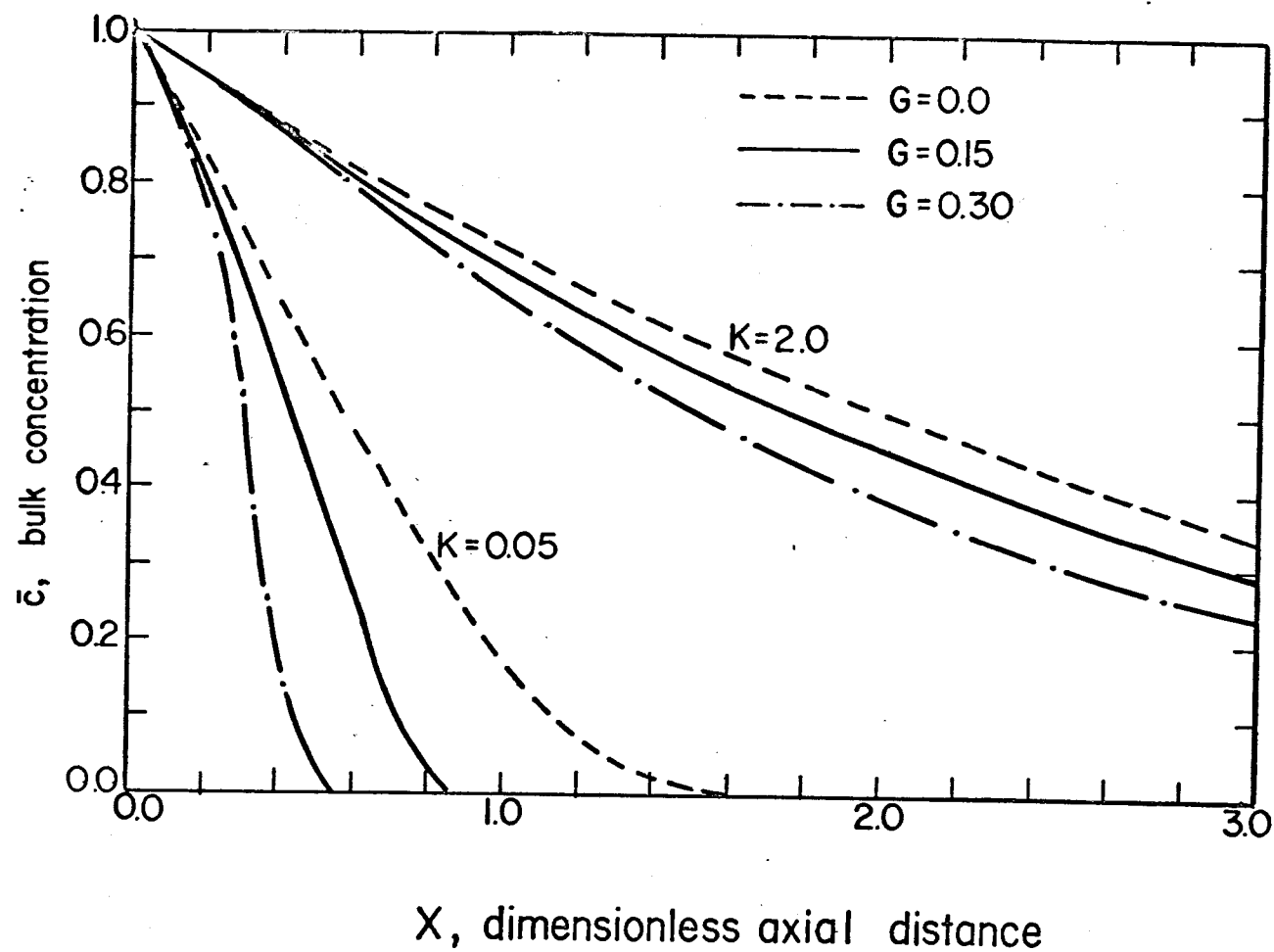
NOTATIONS

A	frequency factor
B	Biot number, hr_o/k
C	dimensionless substrate concentration, S/S_o
C_p	heat capacity of fluid
D_p	molecular diffusivity coefficient
E'	activation energy
E_T	total enzyme concentration
G	dimensionless group of reaction heat generation, $(-H)S_o/\rho C_p T_o$
h	heat transfer coefficient
$- \Delta H$	reaction heat generation
k	thermal conductivity
k_m	Michaelis-Menten constant

K	dimensionless Michaelis-Menten constant, k_m/S_o
r	radial coordinate
r_o	radius of tubular reactor
R	dimensionless radial coordinate, r/r_o
R _g	gas constant
S _g	substrate concentration
S _o	inlet substrate concentration
T	temperature
T _o	inlet temperature
\bar{u}	local fluid velocity
u	average velocity
W	dimensionless frequency factor group, $AE_t r_o^2 / DS_o$
x	axial coordinate
X	dimensionless axial coordinate, $xD / 2r_o^2 \bar{u}$
β	dimensionless activation energy group, $E' / R_g T_o$
ρ	density of mixture
θ	dimensionless temperature, T/T_o

LITERATURES CITED

1. Carbonell, R. G. and Kostin, M. D. Enzyme Kinetics and Engineering. AIChE J., Vol. 18, No. 1, pp. 1-12 (1972).
2. Kobayashi, T. and Moo Young, M. Backmixing and Mass Transfer in the Design of Immobilized-Enzyme Reactors. Biotechnology and Bioengineering, Vol. 13, No. 6, pp. 893-910 (1971).
3. Lin, S. H. Enzyme Reaction in a Tubular Reactor with Laminar Flow. Term Project Report for the course "Special Topic in Biochemical Engineering," Department of Chemical Engineering, Kansas State University, 1971.



Effects of dimensionless Michaelis-Menten constant and dimensionless reaction heat generation group on the bulk substrate concentration

ESTIMATION OF PARAMETERS IN POPULATION MODELS
FOR SCHIZOSACCHAROMYCES POMBE FROM CHEMOSTAT DATA

Gregory C. Martin
Department of Chemical Engineering
University of Nebraska-Lincoln
Lincoln, Nebraska 68508

This work is an extension of that reported earlier¹. More complete details may be found in a forthcoming article.²

Size distributions of chemostat populations of the fission yeast Schizosaccharomyces pombe were obtained previously¹ by use of a Coulter aperture and associated electronics in an attempt to determine the growth kinetics of single cells under nutrient limitation. Equations for doing this were derived by Eakman et al.³ and are shown in Figure 1.

At the time of the earlier presentation¹, models for two different types of single cell growth

$$r = \frac{dm}{dt} = \beta \quad \text{linear}$$

$$f = \frac{dm}{dt} = \gamma_m \quad \text{exponential}$$

had been used with the equations in Figure 1 to fit size distributions at six different holding times. Four different parameters were varied by regression with Marquardt's technique⁴:

m_c - mean cell division size

ϵ - standard deviation of the mother cell size distribution $\times \sqrt{2}$.

ζ - standard deviation of the daughter cell size distribution $\times \sqrt{2}$.

β or γ - linear or exponential rate coefficients, respectively.

In the present work the previous results were modified by a more accurate removal of noise data from the experimental cell size distributions. In addition, two other growth models were investigated:

$$r = \frac{dm}{dt} = \alpha/m \quad \text{inverse}$$

$$r_1 = \beta$$

$$r_2 = 0.2\beta$$

$$1/2m' \leq m \leq \delta m'$$

$$\delta m' \leq m \leq m'$$

} approximate sigmoidal

For the inverse model α replaced β or γ as the fourth parameter varied by regression. In the approximate sigmoidal model δ , the cell sizes at which the growth rate decreased to one-fifth its previous value, was used as a fifth parameter.

Results of the regressions on the four or five parameters for each of the four models at each of the six holding times are as follows. No matter which model is used m_c remains strikingly steady at each holding time with values of 60 to 80 x 10⁻¹² cm³/cell. Values of ϵ , on the other hand, increase steadily with holding time to levels well above those of m_c . Values of ζ , however, are small--rarely larger than 10% of m_c --at all holding times for each model. The rate coefficient, being allowed to vary so that the best fits of the experimental cell size distributions are obtained, generally reaches values lower than those expected for the corresponding hold times and mean cell sizes. However, preliminary work indicated that larger changes in the growth coefficient did not alter the fit markedly. The fifth parameter, δ , generally was between .85 and .9 of the division size.

The F test for the four different models (Table 1) showed that linear and approximate sigmoidal models gave acceptable fits in a majority of cases. One holding time (11.64 hours) could not be submitted to this test because only one sample was taken, but in that case a residual sum of squares showed the linear model fit best.

A plot of experimental and calculated results for a typical case is included (Figure 2).

Additional Notation

\tilde{C}_{Sk}	steady state concentration of limiting nutrient.
m	cell size
m'	cell division size
P	density of daughter cell size distribution
\tilde{w}	steady state concentration of cells of a specific size
Γ'	specific probability of fission
θ	hold time

References

1. I.R. Kothari, P.J. Reilly, P.J. Martin, and J.M. Eakman, 162nd ACS National Meeting, Sept. 1971.
2. I.R. Kothari, G.C. Martin, P.J. Reilly, P.J. Martin, and J.M. Eakman, Biotech. Bioeng. (in press).

3. J.M. Eakman, A.B. Fredrickson, and M.H. Tsuchiya, Chem. Eng. Prog. Symp. Sci. 62(69), 37 (1966).
4. D.W. Marquardt, J. Soc. Ind. Appl. Math., 11, 431 (1963).

Table 1

F Test for Different Models

Model		Inverse		Linear		Sigmoidal		Exponential	
d.f. lack-of-fit		252		252		251		252	
θ , hr	d.f. error	F	%	F	%	F	%	F	%
4.18	256	1.50	100	1.80	100	1.58	100	1.97	100
4.70	512	7.11	100	0.36	0	1.04	65	1.36	100
5.96	512	6.59	100	1.06 (1)	71	0.88 (1)	12		
				1.20 (2)	95	0.96 (2)	37	2.22	100
7.41	512	2.54	100	1.16	92	1.00	49	3.72	100
19.10	512	2.79	100	0.40	0	1.47	100	1.32	100

Figure 1

CELL MASS DISTRIBUTION

$$\frac{d\tilde{w}}{dm} = \frac{2}{r(m, \tilde{C}_{sk})} \int_m^{\infty} \Gamma'(m', \tilde{C}_{sk}) \tilde{w}(m') p(m, m') dm'$$

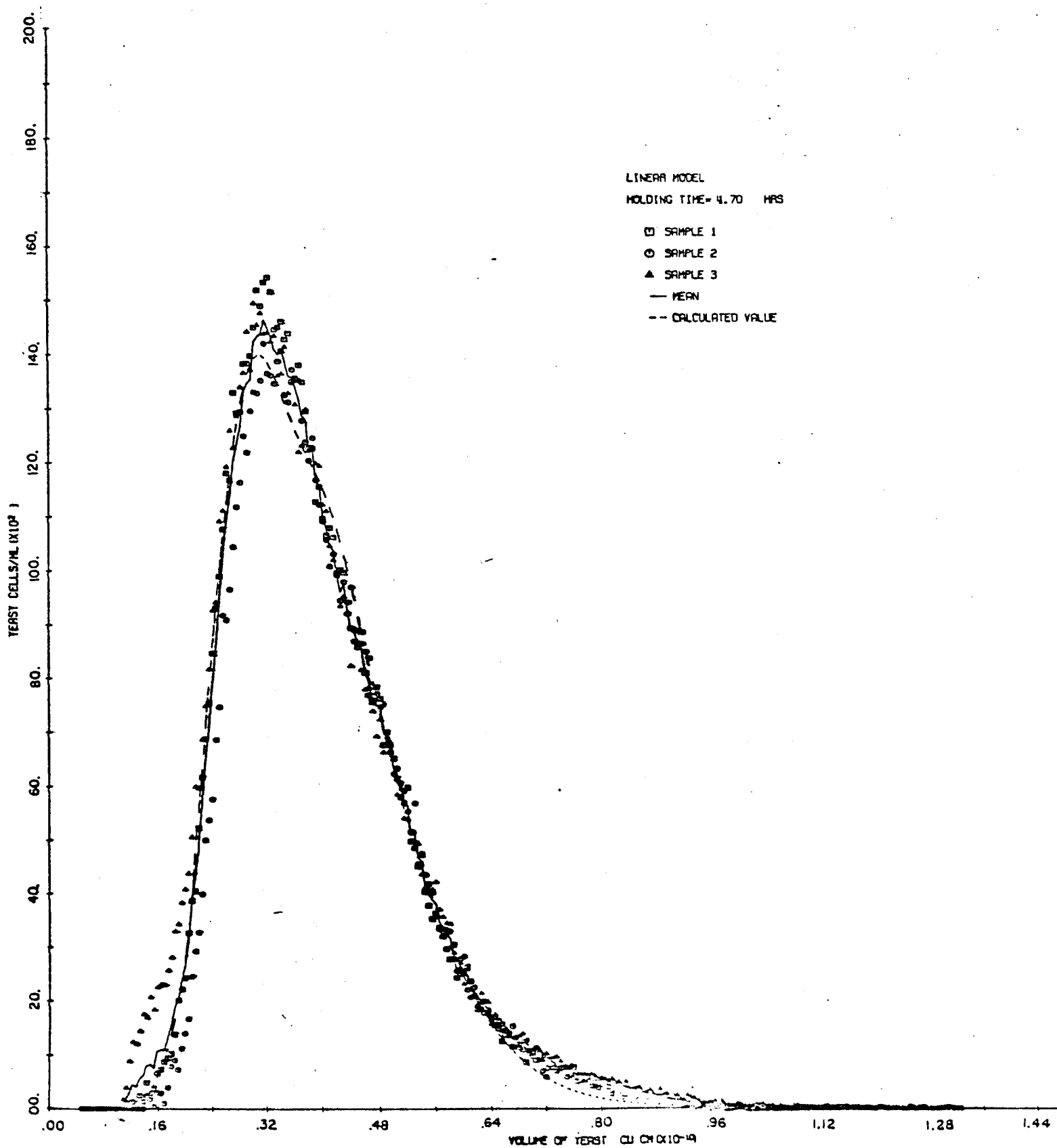
$$- \frac{1}{r(m, \tilde{C}_{sk})} \left[\frac{1}{\theta} + \Gamma'(m, \tilde{C}_{sk}) + \frac{dr}{dm} \right] \tilde{w}(m)$$

WHERE

$$\Gamma'(m, \tilde{C}_{sk}) = \frac{2e^{-\left(\frac{m-m_c}{\epsilon}\right)^2} r(m, \tilde{C}_{sk})}{\epsilon/\pi \operatorname{erfc}\left(\frac{m-m_c}{\epsilon}\right)}$$

$$p(m, m') = \frac{e^{-\left(\frac{m-1/2 m'}{\zeta}\right)^2}}{\zeta/\pi \operatorname{erf}\left(\frac{m'}{2\zeta}\right)}$$

Figure 2



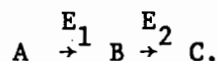
Immobilized Enzymes: Analysis of Ultrafiltration Reactors

J. S. Shastri and P. N. Mishra
 Department of Chemical Engineering
 Kansas State University
 Manhattan, KS 66502

INTRODUCTION

Water insoluble enzyme derivatives offer many advantages in carrying out enzyme catalyzed biological reactions. In vivo, enzyme reactions are heterogeneous as most of the enzymes, in their natural environment, are bound to membranes made up of proteins and lipids. Water-insoluble enzyme derivatives make it possible to study the enzyme behavior in their natural environment. Attaching enzymes to solid supports also facilitates complete recovery of the catalysts and increases the stability of the enzyme to adverse pH and temperature conditions but, unlike the enzymes in solution, have lower activity. A number of methods are available for insolubilizing enzymes¹⁻⁴; these range from crosslinking with bifunctional reagents to physical adsorption on the polymer beads. The object of this paper is to develop some kinetic models to describe the enzyme-catalyzed reactions and 'select' the best possible reactor setup for carrying out this reaction.

The enzyme reaction investigated in this study is the series reaction with two enzymes E_1 and E_2 ; which can be represented as



Constant temperature conditions are assumed in this analysis but extension to non-isothermal reactor is straight forward. The effect of pH on this reaction can be determined from the detailed mechanism of the reaction shown in Fig. 1. Each of the enzymes E_1 and E_2 will be affected by the hydrogen ion concentration in their microenvironment which can be calculated from the bulk pH, if ψ the electrostatic potential is known. In this investigation the substrates and the product are assumed to be uncharged, hence there will not be any transfer of the substrates into the microenvironments of the two enzymes due to electrical forces. It should be noted here that enzymes E_1 and E_2 are required for this reaction and both of these need to be placed on solid supports; this can be done in two different ways. Each of the enzymes could be placed on different solid supports to get a two particle system or both the enzymes could be insolubilized on the same polymer bead in the polyfunctional catalyst system. If a is specific area for the polymer beads and γ is the fraction of beads with enzyme 1, for the two particle system effective areas for the two enzymes are

$$\begin{aligned} a_1 &= \gamma a \\ \text{and } a_2 &= (1 - \gamma)a. \end{aligned} \tag{1}$$

In the polyfunctional case, however, the effective enzyme concentrations will be

$$\begin{aligned} E_1^o &= \gamma E^o \\ \text{and } E_2^o &= (1 - \gamma)E^o \end{aligned}$$

It is also assumed that the reaction is carried out in an ultrafiltration reactor which is operated like a CSTR and the material balance equations are written down for both the catalyst systems (Fig. 2). The mass transfer of the substrate from the bulk phase to the reaction site on the polymer beads is taken as the rate controlling mechanism.

SIMULATION

The above kinetic model was simulated using a digital computer and a parameteric study of various important parameters was carried out. These studies showed that for smaller specific surface areas of the polymer, polyfunctional catalyst gives superior performance and a higher concentration of C in the product. Simulation results also showed that for the two particle individual pH optima can be maintained for each of the two enzymes whereas for the polyfunctional systems only one pH can be maintained. These results showed that polyfunctional system gives better productitivity under certain conditions but there are other factors like mass transfer coefficient k_L , the fraction of enzyme 1 γ_1 and porosity ϵ which make the two particle system superior. The problem of selection of reactors is examined next.

REACTOR SELECTION

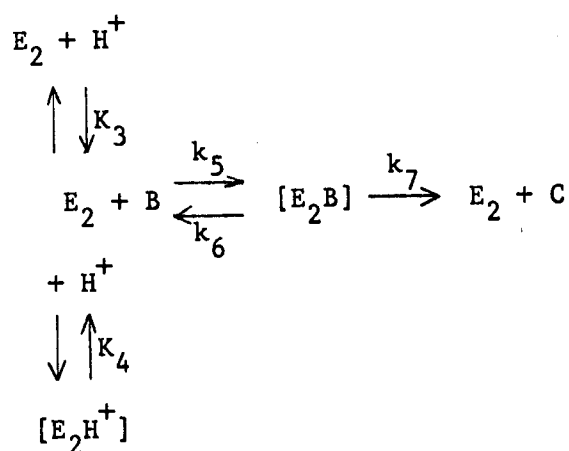
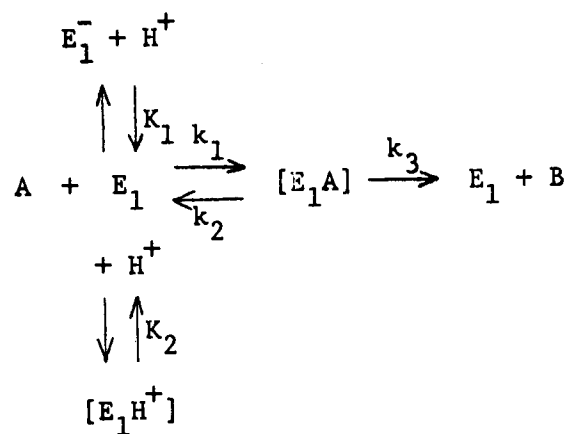
Systems synthesis techniques⁵⁻⁷ are specifically designed to obtain the optimal reactor setup which will maximize the productivity. Two different reactors, with two particle and polyfunctional enzymes are combined in all possible ways (Fig. 3) by introducing the structural parameters α 's. Optimization with respect to the structural parameters and other chosen decision variables will not only optimize the system performance but also the system structure. In the current investigation simplex pattern search procedure was used to optimize the system. The results are reported elsewhere⁸.

CONCLUDING REMARKS

Kinetic models for enzyme reactors can be developed by using the conventional catalyst type of work reported in the chemical engineering literature. Simulation results show that a lot of experimental work is required before advanced models can be developed. Charged substrate can be examined in which case ψ 's become important decision variables. Inclusion of temperature in the list of decision variables creates additional problems of heat transfer, enzyme stability and increase in rate constants.

REFERENCES

1. Carbonell, R. G. and M. D. Kostin, *AIChE Journal* **18** (1), 1 (1972).
2. Melrose, G. J. H., *Rev. Pure and Appl. Chem.*, **21**, 83 (1971).
3. McLaren, A. D. and L. Packer, *Adv. Enzymol.*, **33**, 245 (1970).
4. Kay, L., *Process Biochemistry*, **3**, 36 (1968).
5. Ichikawa, A. and L. T. Fan, to be published in *Chem. Engg. Sci.* (1972).
6. Umeda, T., A. Hirai and A. Ichikawa to be published in *Chem. Engg. Sci.* (1972).
7. Ichikawa, A., N. Nishida and T. Umeda presented at the 34th Annual meeting of the Society of Chem. Engrs. of Japan, Tokyo (1969).
8. Shastri, J. S., P. N. Mishra and L. E. Erickson, Manuscript under preparation (1972).



$$\frac{d[A]}{dt} = \frac{-k_3[E_1]_T[A]}{\frac{k_2}{k_1}\left[1 + \frac{K_1}{H^+} + \frac{H^+}{K_2}\right] + [A]}$$

$$\frac{d[B]}{dt} = \frac{k_3[E_1]_T[A]}{\frac{k_2}{k_1}\left[1 + \frac{K_1}{H^+} + \frac{H^+}{K_2}\right] + [A]} - \frac{k_7[E_2]_T[B]}{\frac{k_6}{k_5}\left[1 + \frac{K_3}{H^+} + \frac{H^+}{K_4}\right] + [B]}$$

Fig. 1. Mechanism of the Enzyme Reaction Examined with Related Kinetic Equations

Case I. Two enzymes, each on different supports; uncharged substrate

$$F_0[A_0] - F_0[A] - K_L a_1([A] - [A_1])V_R = 0$$

$$K_L a_1([A] - [A_1]) = \frac{k_3[E_1]\gamma(1-c)[A_1]}{K'_M + [A_1]}$$

$$K'_M = \frac{k_2}{k_1} \left(1 + \frac{K_1}{H^+} + \frac{H_1^+}{K_2}\right)$$

$$H_1^+ = H^+ e^{-\alpha F \psi_1 / RT}$$

Case I. Balances on [B]

$$F_0([B_0] - [B]) - K_L a_1([B] - [B_1])V_R - K_L a_2([B] - [B_2])V_R = 0$$

$$K_L a_1([B] - [B_1]) + \frac{k_3[E_1]\gamma(1-c)[A_1]}{K'_M + [A_1]} = 0$$

$$K_L a_2([B] - [B_2]) - \frac{k_7[E_2](1-\gamma)(1-c)[B_2]}{K'_S + [B_2]} = 0$$

$$K'_S = \frac{k_6}{k_5} \left(1 + \frac{K_3}{H_2^+} + \frac{H_2^+}{K_4}\right)$$

$$H_2^+ = H^+ e^{-\alpha F \psi_2 / RT}$$

Case II. Polyfunctional catalyst; uncharged substrate.

$$F_0[A_0] - F_0[A] - K_L a([A] - [A_1])V_R = 0$$

$$K_L a([A] - [A_1]) = \frac{k_3[E_1^0](1-c)[A_1]}{K'_M + [A_1]} = 0$$

$$K'_M = \frac{k_2}{k_1} \left(1 + \frac{K_1}{H_1^+} + \frac{H_1^+}{K_2}\right)$$

$$H_1^+ = H^+ e^{-\alpha F \psi_1 / RT}$$

Case II. Balances on [B]

$$F_0[B_0] - F_0[B] - K_L a([B] - [B_1])V_R = 0$$

$$K_L a([B] - [B_1]) + \frac{k_3[E_1^0](1-c)[A_1]}{K'_M + [A_1]} - \frac{k_7[E_2^0](1-c)[B_1]}{K'_S + [B_1]} = 0$$

$$K'_S = \frac{k_6}{k_5} \left(1 + \frac{K_3}{H_1^+} + \frac{H_1^+}{K_4}\right)$$

$$H_1^+ = H^+ e^{-\alpha F \psi_1 / RT}$$

Fig. 2. Material Balances for Two Particle and Polyfunctional Catalyst Reactors

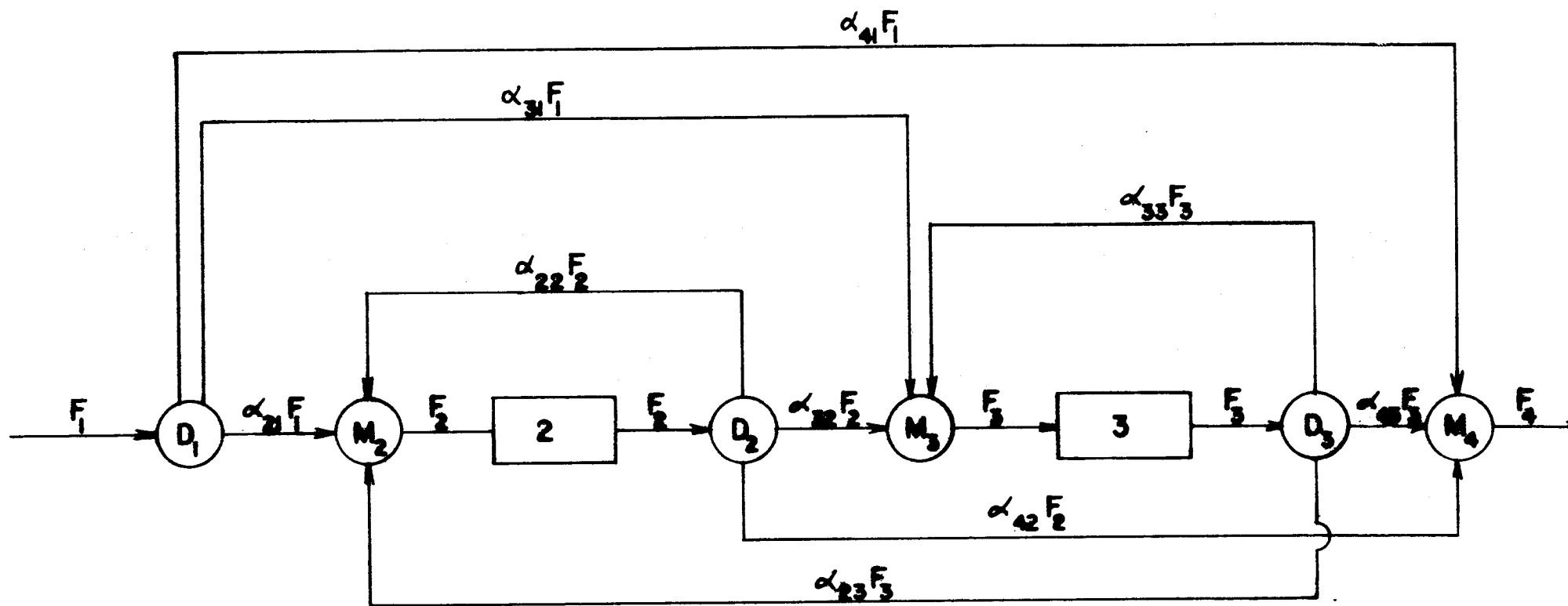


Fig. 3. Systems Synthesis of a two unit enzyme reactor system.

(D) = Distributor, (M) = Mixer

MODELLING UNSTEADY-STATE TWO-SPECIES DATA
USING RAMKRISHNA'S STALING MODEL

Mark D. Young
Department of Chemical Engineering
University of Nebraska-Lincoln
Lincoln, Nebraska 68508

This work is an extension of that performed by C. C. Chao¹ on the two-species culture of the bacterium Acetobacter suboxydans and the yeast Saccharomyces carlsbergensis in a chemostat. It was supposed that these organisms interact in a commensalistic relationship where A. suboxydans oxidizes mannitol to fructose while fructose is the energy source for S. carlsbergensis. The commensalistic nature is exhibited by S. carlsbergensis depending upon A. suboxydans for its energy source while the latter is independent of the former.

Chao obtained data on mannitol, fructose, bacterial, and yeast concentration for the dynamic response of the system to a step change in dilution rate. The response was unexpectedly erratic, with oscillations of varying size and period eventually coming to a new steady state. This led to the presumption that the bacteria were inhibited by a substance excreted by the yeast.

It is, therefore, the purpose of this work to obtain a simple mathematical model containing inhibitor effects that will adequately fit the data obtained. The model selected is the third staling effect model developed by Ramkrishna² for single species culture. This model was chosen because it is fairly general and easily provides a means of interaction for two-species culture through the secretion of inhibitors. It is easily adopted to the purpose at hand and it can be restricted to simpler models by setting certain rate constants and coefficients to infinity or zero. The mechanism is given on Figure 1.

The system is being modelled by the Continuous Systems Modelling Program (CSMP) which simulates an analog computer, using the fourth order Runge-Kutta technique for integration. The simultaneous differential equations derived from the model are given on Figure 2.

The unknown quantities to be determined are a_{t_1} , a_{t_2} , a'_{t_1} , a'_{t_2} , a_{n_1} , a_{n_2} , C_1 , C_2 , C'_1 , C'_2 , N_1 , N_2 , and T .

It should be noted that in Chao's work Y_{x_1/s_1} and Y_{x_2/s_2} are not constants. In the present work they are represented as functions of S_1 and S_2 values. The unknown quantities will be obtained by making simplifying assumptions and using trial-and-error values to develop a simple but adequate model.

Notation Used

D Dilution rate.

N_1 Unit of concentration of dead cells of A. suboxydans.

N_2 Unit or concentration of dead cells of S. carlsbergensis.

S_1 Unit or concentration of mannitol.

S_2 Unit or concentration of fructose.

T Unit or concentration of inhibitor.

X_1 Unit or concentration of A. suboxydans.

X_2 Unit or concentration of S. carlsbergensis.

μ_{1max} , μ_{2mas} Maximum specific growth rates of A. suboxydans and S. carlsbergensis, respectively.

All quantities denoted with C are rate constants.

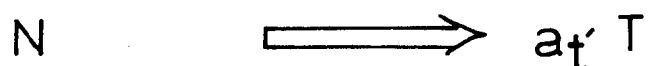
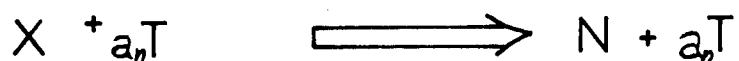
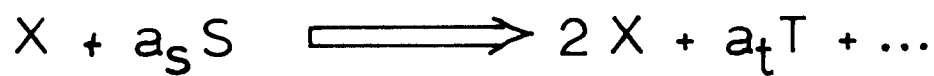
All quantities denoted with a are stoichiometric constants.

Literature Cited

- (1) Chao, C. C. and Reilly, P. J., Biotech. Bioeng., 14, 75 (1972).
- (2) Ramkrishna, D., "Models for the Dynamics of Microbial Growth", Ph.D. thesis, University of Minnesota (1965).

Figure 1

RAMKRISHNA'S MECHANISM



MODIFIED FOR TWO SPECIES

(common inhibitor assumed)

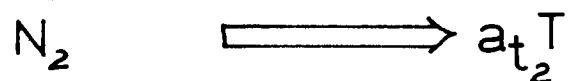
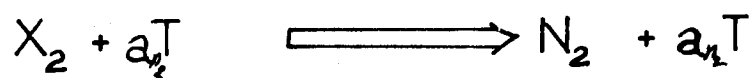
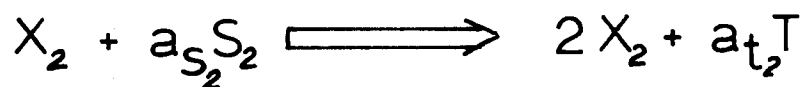
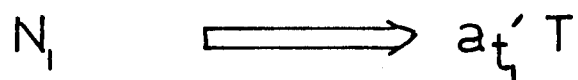
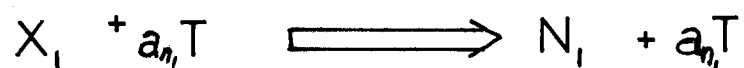
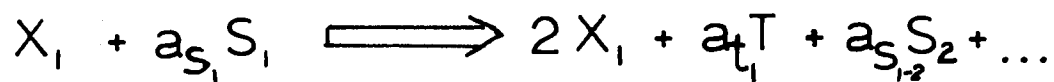


Figure 2

SIMULATION OF SYSTEM IN CONTINUOUS CULTURE

$$\frac{dX_1}{dt} = R_1 X_1 - D X_1$$

$$\frac{dX_2}{dt} = R_2 X_2 - D X_2$$

$$\frac{dS_1}{dt} = D(S_{10} - S_1) - R_1 X_1 / Y_{\frac{X_1}{S_1}}$$

$$\frac{dS_2}{dt} = Y_{\frac{S_2}{X_2}} R_1 X_1 - D S_2 - R_2 X_2 / Y_{\frac{X_2}{S_2}}$$

$$\frac{dT}{dt} = a_{t_1} X_1 R_1 + a'_{t_1} C_1 N_1 + a_{t_2} X_2 R_2 + a'_{t_2} C_2 N_2 - D T$$

$$\frac{dN_1}{dt} = a_{n_1} C_1 X_1 T - C_1 N_1 - D N_1$$

$$\frac{dN_2}{dt} = a_{n_2} C_2 X_2 T - C_2 N_2 - D N_2$$

$$R_1 = \frac{\mu_{1max} S_1}{C_{S_1} + S_1} - C_1' T$$

$$R_2 = \frac{\mu_{2max} S_2}{C_{S_2} + S_2} - C_2' T$$

Optimization of Step Aeration Waste Treatment System Using EVOP

George C. Y. Chu

Kansas State University

Much effort has been devoted to theoretical studies of step aeration waste treatment systems (1,2,3,4). However, little experimental work has been done to search and develop an optimum step aeration process.

The present study is based on a two-tank step aeration treatment system with recycle of the active sludge. EVOP (Evolutionary Operation) search techniques are introduced to seek the optimum plateau (5). The ratio of the inlet flow rates into the two tanks and the ratio of the volumes of the first and second tanks are the two decision variables for EVOP. The total COD in the effluent is the objective function of the operation which will be minimized.

Three series of experiments were carried out following the EVOP design. In the first series of experiments, the volume ratio ranged from 0.25 to 0.75 and the flow rate ratio ranged from 0.40 to 0.80. The second series, which repeated the first series, was conducted to investigate the reproducibility of the results. The third series of experiments covered the range of values from 0.35 to 0.65 for the volume ratio and from 0.50 to 0.70 for the flow rate ratio. Each experiment was conducted for a time sufficiently long so that a reliable estimation of the steady state could be made. Factors such as temperature ($25 \pm 0.5^\circ\text{C}$), pH (6.8 ± 0.4), and aeration rate (2.0 VVM) were controlled for the process so as to minimize their effect on system behavior. The cell dry weight (by Millipore filtration) and substrate concentration in terms of COD (by dichromate method) (6) were measured.

Table 1 shows the results of the three series of experiments. An analysis of the results obtained using EVOP has been carried out and is shown in Table 2. From the results of the first two series of experiments the operating condition with volume ratio of 0.5 and flow rate of 0.6 gives the highest total COD removal. In the third series of experiments the range of volume ratio and flow rate ratio were reduced to see if improved performance could be found near this best operating condition. The results of the third series of experiments show that the highest total COD removal (82.0%) is under the operating condition with volume ratio of 0.50 and flow rate ratio of 0.60.

This study shows that if the total volume and total influent waste flow rate are fixed in a two-stage step aeration waste treatment system with recycle, the operating condition, which is the combination of the volume ratio and the inlet flow rate ratio does have a significant influence upon the treatment efficiency of the waste treatment system. The EVOP method appears to be useful in optimizing the operation of biological waste treatment systems.

The details of this work are presented elsewhere (7).

References

1. Gould, R.H., Sewage Works J., 14, 1, 70 (Jan., 1942).
2. Polonscik, S., R.B. Grieves and W.O. Pipes, Proceedings of the 20th Industrial Waste Conference, May, 1965, Purdue University, Lafayette, Ind. (1966).
3. Erickson, L.E. and L.T. Fan, J. Water Pollution Control Federation, 40, 345 (1968).
4. Erickson, L. E., Y.S. Ho and L.T. Fan, *ibid*, 40, 717 (1968).
5. Box, G.E.P. and N.R. Draper, "Evolutionary Operation: A Statistical Method for Process Improvement," John Wiley and Sons, Inc., New York (1969).
6. "Standard Method for the Examination of Water and Waste Water," 12th ed., American Public Health Association, Inc., (1965).
7. Erickson, L.E., Report Contribution No. 90, Kansas Water Resources Research Institute, Manhattan, Kansas (1972).

Table 1. Performance of Treatment System

Series No. 1	Operating Condition	$\bar{V}^* = 0.25$ $\bar{Q}^{**} = 0.40$	$\bar{V} = 0.75$ $\bar{Q} = 0.80$	$\bar{V} = 0.25$ $\bar{Q} = 0.80$	$\bar{V} = 0.75$ $\bar{Q} = 0.40$	$\bar{V} = 0.50$ $\bar{Q} = 0.60$
	Total COD Removal (%)	70.40	73.39	69.35	55.42	75.93
Series No. 2	Operating Condition	$\bar{V} = 0.25$ $\bar{Q} = 0.40$	$\bar{V} = 0.75$ $\bar{Q} = 0.80$	$\bar{V} = 0.25$ $\bar{Q} = 0.80$	$\bar{V} = 0.75$ $\bar{Q} = 0.40$	$\bar{V} = 0.50$ $\bar{Q} = 0.60$
	Total COD Removal (%)	68.79	69.80	67.42	56.96	71.47
Series No. 3	Operating Condition	$\bar{V} = 0.35$ $\bar{Q} = 0.50$	$\bar{V} = 0.65$ $\bar{Q} = 0.70$	$\bar{V} = 0.35$ $\bar{Q} = 0.70$	$\bar{V} = 0.65$ $\bar{Q} = 0.50$	$\bar{V} = 0.50$ $\bar{Q} = 0.60$
	Total COD Removal (%)	69.74	74.36	73.95	69.48	82.00

* \bar{V} = Volume ratio = $\frac{V_1}{V_1 + V_2}$; $V_1 + V_2 = 2.4$ liters.

** \bar{Q} = Flow ratio = $\frac{Q_1}{Q_1 + Q_2}$; $Q_1 + Q_2 = 25$ ml/min.

Table 2. EVOP information board of total COD removal.

Series No.		1	3
Operating range		\bar{V} : 0.25 to 0.75 \bar{Q} : 0.40 to 0.80	\bar{V} : 0.35 to 0.65 \bar{Q} : 0.50 to 0.70
Process averages		<div><div>\bar{V}</div><div><div>55.42 73.39</div><div>75.93</div><div>70.40 69.35</div><div>\bar{Q}</div></div></div>	<div><div>\bar{V}</div><div><div>69.48 74.36</div><div>82.00</div><div>69.74 73.95</div><div>\bar{Q}</div></div></div>
2 S.E. limit for averages		± 7.12	± 4.52
Effects with 2 S.E. limits	Phase mean	68.89	73.90
	\bar{Q}	8.46 ± 7.12	4.54 ± 4.52
	\bar{V}	-5.47 ± 7.12	0.08 ± 4.52
	$\bar{Q} \times \bar{V}$	9.51 ± 7.12	0.34 ± 4.52
	Change in mean	-7.04 ± 6.37	8.10 ± 4.04
Estimated standard deviations		7.96	5.05

GROWTH OF THE BLUE-GREEN ALGA MICROCYSTIS

AERUGINOSA UNDER DEFINED CONDITIONS

Shinji Goto

Department of Chemical Engineering
University of Nebraska-Lincoln
Lincoln, Nebraska 68508

The eutrophication of lakes has become a serious problem, especially in the Great Plains states. Its causes and methods of prevention remain highly controversial. In the last several years, there has been considerable speculation that eutrophication is aggravated by phosphates and nitrates released from fertilized fields and incompletely treated sewage.

Recently L. E. Kuentzel¹, after conducting a exhaustive literature survey, has suggested that availability of carbon dioxide often limits algal growth, and therefore most cases of massive algal blooms in lakes are caused by carbon dioxide released by bacteria growing on organic pollution. In general, it is observed that massive increases in the number of bacteria always accompany massive algal blooms.

He further stated that there were three sources for the CO₂ used by algae. The first is the atmosphere, but this source is² limited by slow mass transport across the air-water interface. The second is the abstraction of bicarbonate ions dissolved in the water, but this quickly causes the pH to rise above the value at which the algae can grow. The third, which he considers to be the major source, is bacterial excretion. Since aerobic bacteria require oxygen to degrade organic matter and produce carbon dioxide, while algae require carbon dioxide to photosynthesize organic matter and produce oxygen, a symbiotic system can be established that supplies sufficient CO₂ to the algae.

This research will therefore attempt to determine the limiting factors for growth of the blue-green alga Microcystis aeruginosa, which causes massive algal blooms in lakes, by growing it in continuous culture under controlled conditions. Eventually this project will evaluate the symbiotic growth of a typical species of bacteria with M. aeruginosa.

Media and Microbial Strains

An obligately aerobic bacterial species which produces only CO₂ and water and can grow in a medium suitable for the algae when small amounts of glucose were added was desirable. For this

reason, Pseudomonas aeruginosa NRRL-B800 was chosen for further study.

Two strains of M. aeruginosa, NRC-1 from Prof. P. R. Gorham of the University of Alberta and Wisconsin 1036 from Prof. G. C. Gerloff, were obtained. Neither had been freed of bacteria.

By experimentation with the impure strains ASM-1 medium² was chosen over ASM³ and PAAP⁴. TRICINE at 10mM concentration was selected for use as a buffer over TRIS, BICINE, and TAPS. The temperature and pH for algal growth were set at 23 ~ 24°C and 8.0 ~ 8.5, respectively.

Algal Purification

Unicoccal blue-green algae have historically been difficult to purify because they grow poorly on solid media. Therefore two approaches to the purification of the two strains of M. aeruginosa were taken. In the first method, varying concentrations of six antibiotics, both singly and in combination, were used to attempt to kill the contaminating bacteria without killing all the algae. While it was possible to increase the ratio of algae to bacteria significantly, it was not possible to effect a successful isolation.

In the second method, the impure cultures were streaked on Petri dishes with ASM-1 medium containing 1.5% of agar sterilized separately⁵. Sterilized glass capillaries were employed to transfer pure algal colonies to test tubes containing 2-3 ml ASM-1 medium. This method was tedious, because most of the algal colonies, which were very small, were covered with contaminating bacterial colonies. Usually there was no growth in liquid culture and when there was, generally it was contaminated; but eventually by this method two pure algal cultures of 1036 and one of NRC-1 were obtained.

The maximum growth rates in shaker flasks for pure 1036 and NRC-1 were each 0.016 hr⁻¹.

Continuous Culture of the Pure Algae

Once the algae were purified, it was possible to grow the pure cultures in a 5-liter New Brunswick fermentor system so that limiting concentrations of major nutrients could be determined under controlled conditions. It was found necessary to first fabricate the fermentor internals of Teflon, since the original stainless steel internals were toxic to the algae.

Continuous culture of the pure algae is being studied by varying the flow rate, feed nutrient concentrations such as

phosphate and nitrate, light intensity, and air or enriched carbon dioxide flow rate. Samples will be analyzed for optical density, cell concentrations by using the Coulter counter, and phosphate, nitrate, oxygen, and carbon dioxide concentrations, the latter two with an in situ oxygen electrode and a carbon dioxide electrode in the exit line.

Further experimentation will observe the concurrent growth of M. aeruginosa and P. aeruginosa in the chemostat under similar conditions to determine if either species affects the others. It is already apparent that bacteria and algae exchange carbon dioxide and oxygen. The great difficulty in inducing algae to grow in the pure state and the ability of heterotrophic bacteria to grow in an organic-free medium when in the presence of algae led to the presumption that **several** other interactions also occur. A study of the interactions between typical bacterial and blue-green algal species and an determination of the limiting concentrations of essential nutrients for a common nuisance alga should be of use in preventing lake eutrophication.

References

- (1) Kuentzel, L. E., J. Water Pollution Fed., 41, 1737 (1969).
- (2) Gorham, P. R., private communication (1971).
- (3) McLachlan, J., and P. R. Gorham, Can. J. Microbiol., 8, 1, (1962).
- (4) Brenner, T. E., Provisional Algae Assay Procedure (1969).
- (5) Allen, M. M., J. Phycol., 4, 1, (1968).

Acknowledgement

Support for this project was received in full or in part from the Office of Water Resources Research, Department of the Interior, under the Public Law 88-379 program.

Prakash N. Mishra and Ming-ching T. Kuo
Department of Chemical Engineering
Kansas State University
Manhattan, Kansas 66502

INTRODUCTION

A study of the effects on the performance of the activated sludge process system upon the inclusion of a primary clarifier, was the objective of this investigation. The system was simulated on a digital computer using the software package ASPOP (Activated Sludge Process Optimization Program) developed by Fan *et al.* (1 - 3). The influent wastewater to the system was assumed to contain both dissolved organics and suspended solids. Empirical models developed by Voshell and Sak (4) were employed for expressing the primary clarifier performance for the two cases: (i) no addition of a flocculating agent, (ii) addition of a flocculating agent at a fixed dosage.

SYSTEM DESCRIPTION

The activated sludge process system, including the primary clarifier, as considered in this study is shown in Figure 1. The influent flow rate was considered to be constant and the effluent water quality was kept fixed at a set standard in terms of its BOD.

The performance equations for the primary clarifier, the mixing point, the aeration vessel and the secondary clarifier are given in Table 1. In this study it was assumed that the biodegradable fraction of the suspended solids in the primary clarifier effluent can be represented by a constant C_r which generally has a value of 0.7. It was also assumed that the consumption rate of the biodegradable fraction of the suspended solids in the primary clarifier effluent is the same as the consumption rate of the dissolved organic nutrients.

Table 2 gives numerical values of the inlet conditions and the various constants employed in the correlations used. A dispersion model was used as the flow model for the aeration vessel. An empirical correlation developed by Fan *et al.* (1), based on Murphy's experimental data (5), was used to correlate the Peclet number in the aeration vessel to other aeration vessel parameters. The secondary clarifier performance was expressed by a model due to Naito *et al.* (6) on the assumption that plug flow conditions prevail in the secondary clarifier.

RESULTS AND DISCUSSION

Figure 2 shows that the concentration of suspended solids in the primary clarifier effluent is a monotonic increasing function of the concentration of suspended solids in the influent wastewater, as is to be expected. This implies that the suspended solids removal efficiency of the primary clarifier increases with an increase in the concentration of suspended solids in the influent wastewater. Figure 2 also indicates that there is a considerable increase in the suspended solids removal efficiency of the primary clarifier upon the addition of a flocculating agent. Since a large fraction of the suspended solids exerts considerable BOD on the system, the use of a flocculating agent will be advantageous from the secondary system design point of view.

The process loading factor, which is a measure of the pollutant load on the secondary system, is seen to be a monotonic increasing function of the concentration of dissolved and suspended pollutants in the influent wastewater from Figure 3. The addition of a flocculating agent to the primary clarifier tends to bring about an appreciable reduction in the process loading factor. Also an increase in the concentration of microbes in the return sludge reduces the process loading factor, as is to be expected. The process loading factor would be considerably higher if the primary clarifier was not included in the process system.

Figure 4 exhibits the effect of primary clarifier surface area on some of the other system variables. It can be seen that the concentration of suspended solids in the primary clarifier effluent decreases as the primary clarifier surface area increases, but such a decrease will have a limit as can be seen by the decreasing slope of the curve. Such a decrease in the suspended solids concentration in the primary clarifier effluent implies a corresponding decrease in the process loading factor. Increasing the primary clarifier surface area has little effect on the sum of the volumes of the aeration vessel and the secondary clarifier, but the volume of the primary clarifier increases since the primary clarifier depth is kept fixed.

The variations in the volumes of the aeration vessel, the secondary clarifier, and the total system, as functions of the concentration of dissolved and suspended pollutants in the feed sewage is shown in Figure 5. All three volumes are observed to be monotonic increasing functions, as is to be expected due to the increase in the pollutant load on the system. The increase in the aeration vessel volume is not only due to the increase in the amount of nutrients to be metabolized but also due to the increase in the degree of dispersion in the aeration vessel. Figure 5 also exhibits that an increase in the concentration of microbes in the return sludge decreases the volumes of the aeration vessel and the total system but increases the volume of the secondary clarifier. Also, the use of a flocculating agent in the primary clarifier reduces the volumes of the aeration vessel and the total system but has no effect on the secondary clarifier volume.

CONCLUSIONS

This study points out that the inclusion of a primary clarifier into the activated sludge process system is advantageous in the sense that it reduces the pollutant load on the secondary system considerably, especially at high concentration of suspended solids in the influent wastewater. This advantage is realized in terms of the savings in the volume of the aeration vessel, but the corresponding increase in the total system volume due to the additional volume of the primary clarifier more than offsets it. Hence, there may not be a direct economic advantage in using a primary clarifier if one is concerned with only the construction cost of the system. The primary clarifier has many other advantages which have not been mathematically modeled in this study and hence the above conclusions are restrictive. Also, the advantage of using a flocculating agent in the primary clarifier is self evident from the results of this study.

REFERENCES

1. Fan, L. T., L. E. Erickson and G. K. C. Chen, "Computer Optimization of Biological Waste Treatment Processes," CEP Symp. Ser., WATER 1971, in press (1972).
2. Chen, G. K. C., L. T. Fan and L. E. Erickson, "Computer Software Development for Biological Waste Treatment Processes," JWPCF, in press (1972).
3. Fan, L. T., P. N. Mishra, G. K. C. Chen and L. E. Erickson, "Application of Systems Analysis Techniques in Biological Waste Treatment," presented at 4th Int. Ferm. Symp., Kyoto, Japan, (March 1972).
4. Voshel, D., and J. G. Sak, JWPCF, 40(5), Part 1, 203 (1968).
5. Murphy, K. L., "The Significance of Flow Patterns and Mixing in Biological Waste Treatment," presented at ACS Meeting, Chicago (Sept. 1970).
6. Naito, M., T. Takamatsu and L. T. Fan, Water Research, 3, 433 (1969).

ACKNOWLEDGEMENT

Financial support was provided by the Water Quality Office of EPA (Grant 17090 ELL; project leader L. T. Fan).

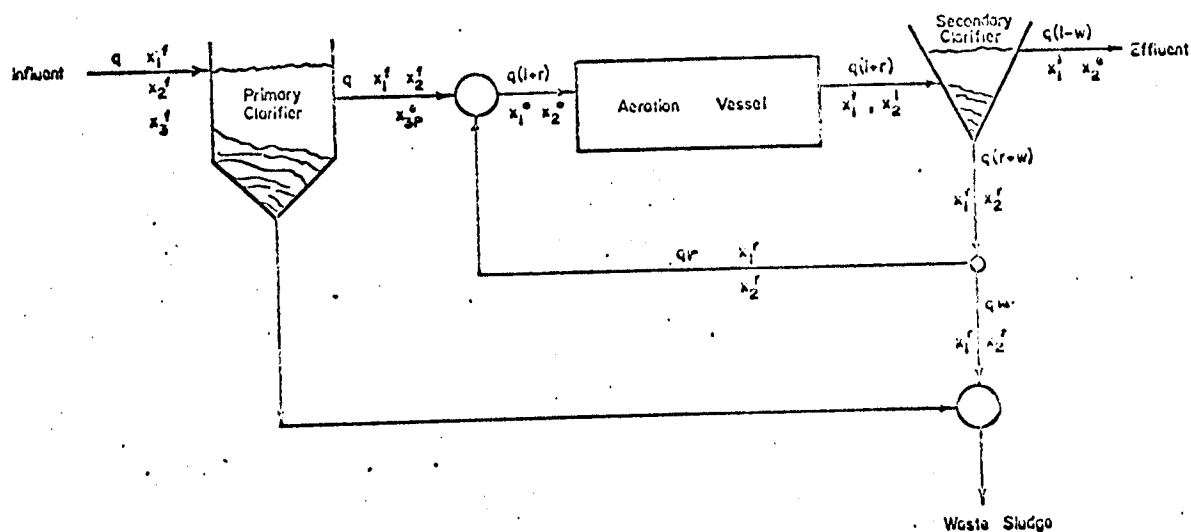


Fig. 1. Schematic Diagram of the Activated Sludge Process System.

NOTATION

A_L	Length of aeration vessel, ft.
A_P	Surface area of primary clarifier, ft ² .
A_S	Surface area of secondary clarifier, ft ² .
A_V	Width of aeration vessel, ft.
C_d	Discharge criterion, ppm.
C_r	Conversion coefficient, ppm BOD/ppm suspended solids.
$i = 1$	Organic nutrients.
$i = 2$	Microbes.
k	Maximum specific growth rate of cells when the substrate concentration is not limiting the growth rate, hr ⁻¹ .
k_D	Specific endogenous microbial attrition rate, hr ⁻¹ .
K	Concentration of substrate at which the observed specific growth rate is one-half the maximum value, ppm.
K_S	Specific constant for secondary clarifier, hr ⁻¹ .
m	Conversion coefficient, ppm BOD/ppm sludge dry weight.
P	Specific constant for secondary clarifier, dimensionless.
Pe	Peclet number for the aeration vessel, dimensionless.
PLF	Process loading factor, lb BOD/lb solids/day.
q	Volumetric flow rate of influent wastewater, MGD.
Q_{Air}	Air flow rate to aeration vessel, scfm/100 ft ³ .
r	Sludge recycle ratio, dimensionless.
R	Reaction number, dimensionless.
T_A	Aeration vessel residence time, hrs.

T_S	Secondary clarifier residence time, hrs.
V_A	Aeration vessel volume, MG.
V_P	Primary clarifier volume, MG.
V_S	Secondary clarifier volume, MG.
V_T	Total system volume, MG.
x_1	Concentration of organic nutrients in aeration vessel, ppm.
x_2	Concentration of microbes in aeration vessel, ppm.
x_1^0	Concentration of organic nutrients entering aeration vessel, ppm.
x_2^0	Concentration of microbes entering aeration vessel, ppm.
x_1^1	Concentration of organic nutrients leaving aeration vessel, ppm.
x_2^1	Concentration of microbes leaving aeration vessel, ppm.
x_2^e	Concentration of microbes in secondary clarifier effluent, ppm.
x_{3p}^e	Concentration of suspended solids in primary clarifier effluent, ppm.
x_1^f	Concentration of dissolved organic nutrients in influent wastewater, ppm.
x_2^f	Concentration of microbes in influent wastewater, ppm.
x_3^f	Concentration of suspended solids in influent wastewater, ppm.
x_1^r	Concentration of organic nutrients in recycle stream to aeration vessel, ppm.
x_2^r	Concentration of microbes in recycle stream to aeration vessel, ppm.
Y	Yield constant.
α	Specific constant for secondary clarifier, dimensionless.
ϕ_1	Organic nutrients consumption rate.
ϕ_2	Microbial growth rate.
η	Dimensionless aeration vessel length.

Table 1

Primary Clarifier	Voshel and Sak Model	Flocculation	$x_{3P}^e = x_3^f \left[1 - \frac{0.7788(x_3^f)^{0.17}}{(q/A_p)^{0.13}} \right]$
		No Flocculation	$x_{3P}^e = x_3^f \left[1 - \frac{0.5675(x_3^f)^{0.27}}{(q/A_p)^{0.22}} \right]$
Mixing Point	Organic Nutrients Balance		$x_1^0 = \frac{1}{1+r} (x_1^f + C_r x_{3P}^e) + \frac{r}{1+r} x_1^r$
	Microorganisms Balance		$x_2^0 = \frac{1}{1+r} x_2^f + \frac{r}{1+r} x_2^r$
Aeration Vessel	Kinetic Model	Organic Nutrients Consumption Rate	$\phi_1 = \frac{dx_1}{dt} = \frac{-k x_1 x_2}{Y(K + x_1)}$
		Microbial Growth Rate	$\phi_2 = \frac{dx_2}{dt} = \frac{k x_1 x_2}{K + x_1} - k_D x_2$
	Peclet Number--Residence Time Relationship		$Pe = \frac{0.3125(A_L/A_H)^2}{T_A(Q_{Air})^{0.346}}$
	Dispersion Model		$\frac{1}{Pe} \frac{d^2 x_1}{d\eta^2} - \frac{dx_1}{d\eta} + R\phi_1 = 0, \quad i = 1, 2$
	Boundary Conditions		at $\eta = 0, \quad \frac{1}{Pe} \frac{dx_1}{d\eta} = x_1 - x_1^0, \quad i = 1, 2$
			at $\eta = 1, \quad \frac{1}{Pe} \frac{dx_1}{d\eta} = 0, \quad i = 1, 2$
Secondary Clarifier	Naito, Takamatsu, Fan Model		$x_2^e = p[x_2^1]^a \exp[-K_S T_S]$

Table 2

$q = 3$ MGD	$x_1^f = 100 - 500$ ppm
$x_2^f = 0$	$x_3^f = 100 - 300$ ppm
$x_1^r = 11$ ppm	$x_2^r = 8,000$ 10,000 ppm 12,000
$r = 0.35$	
$A_L = 150$ ft	$A_P = 5000$ ft ² 2500 - 10,000 ft ²
$D_P = 10$ ft	$A_H = 30$ ft
$Q_{Air} = 21.0$ scfm/ft ³	$D_S = 10$ ft
$k_D = 0.002$ hr ⁻¹	$k = 0.1$ hr ⁻¹
$Y = 0.5$	$K = 100$ ppm
$\alpha = 0.5$	$p = 2.1$
$C_r = 0.7$	$K_S = 0.74$
	Effluent Quality $x_1^1 + m x_2^e = C_d$
	$C_d = 20$ ppm
	$m = 0.5$

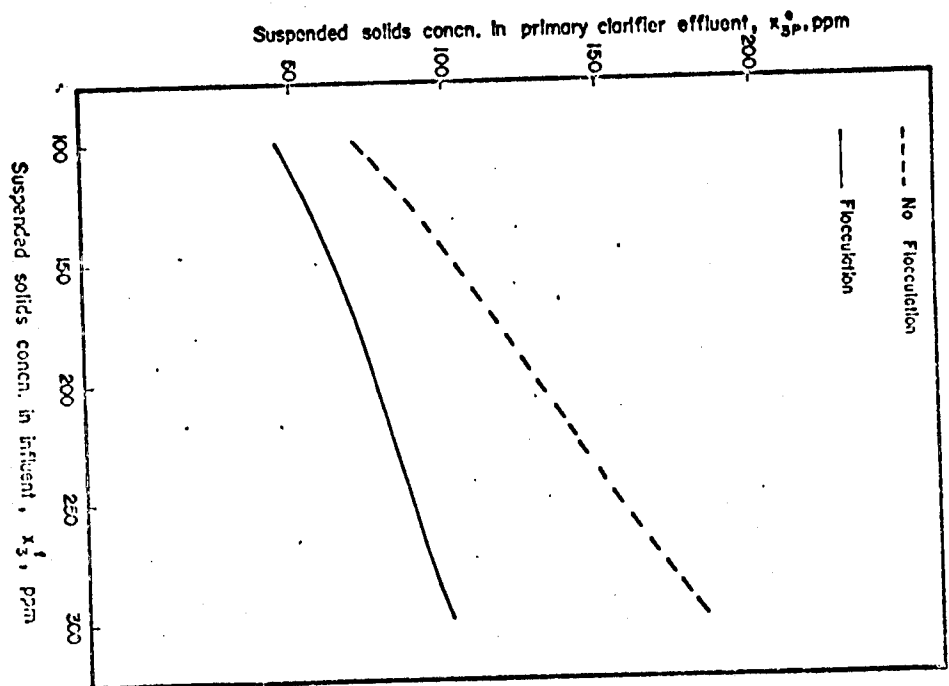


Fig. 2. Variation of x_{3p}^* with x_3' for $q=3$ MGD and $A_p=5000$ ft²

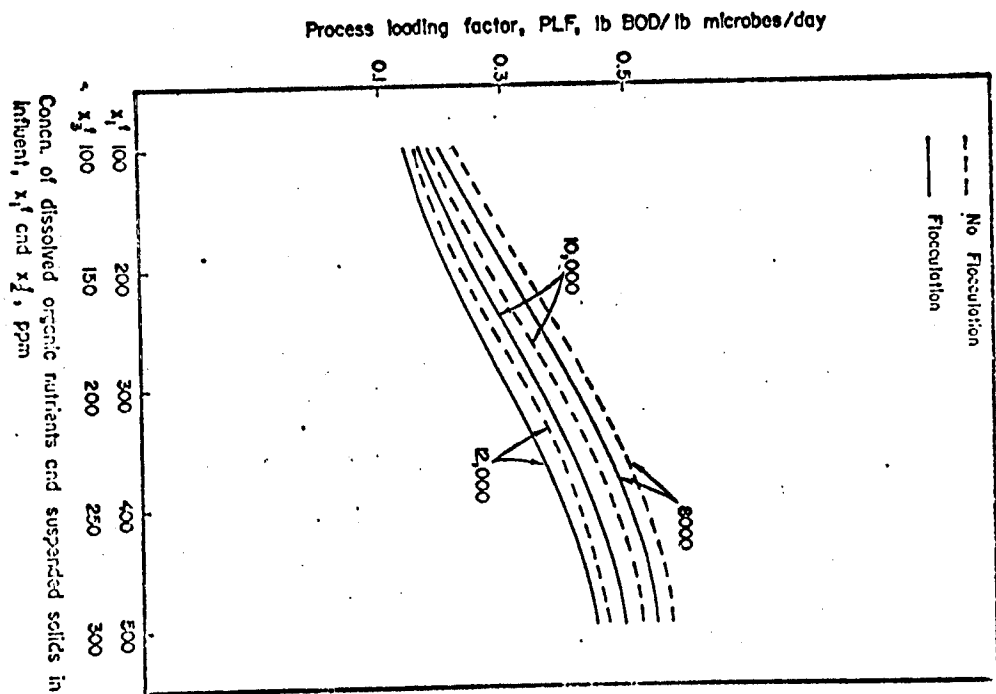


Fig. 3. Variation of PLF with x_1' and x_2' with x_2' as parameter, for $q=3$ MGD and $A_p=5000$ ft²

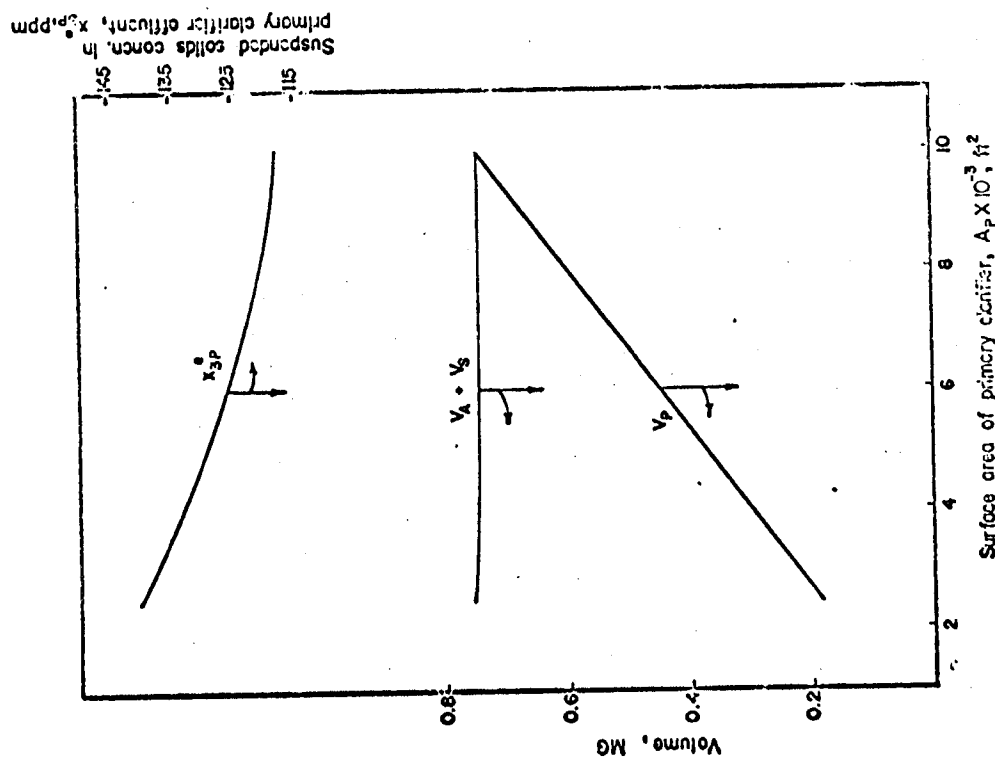


Fig. 4. Variations of x_{3P}^* ($V_A + V_S$) and V_P with A_P for $q=3$ MGD, $x_1^f=300$ ppm, $x_3^f=150$ ppm and $x_2^f=10,000$ ppm, with no flocculation.

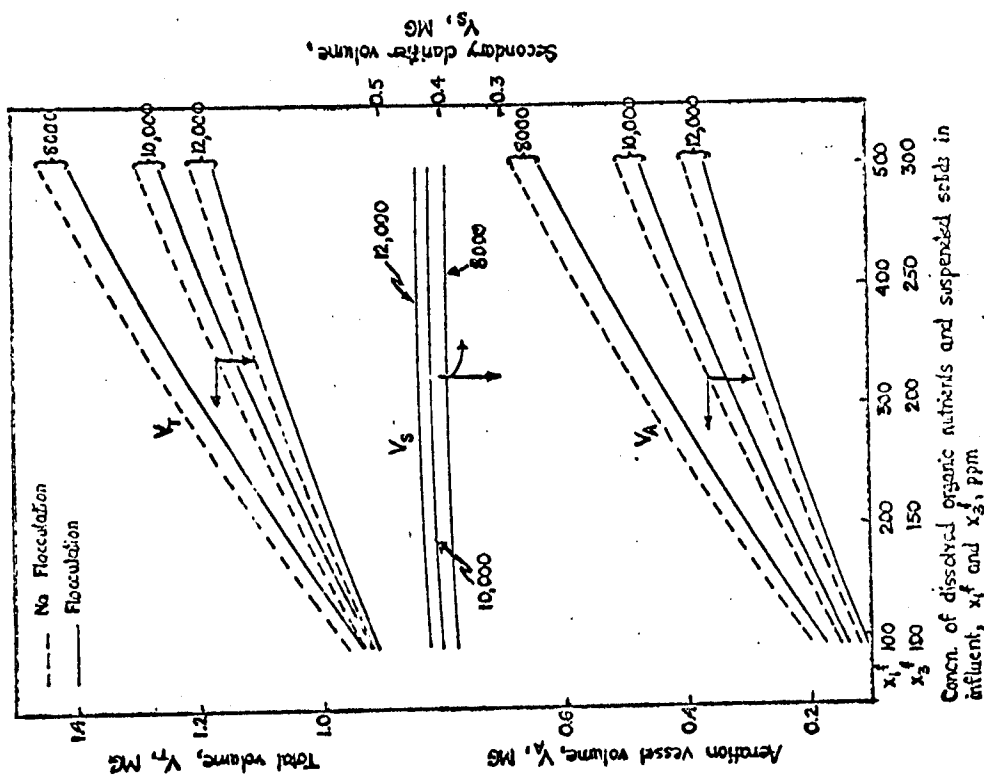


Fig. 5. Variations of V_T , V_S and V_A with x_1^f and x_3^f , for $q=3$ MGD, $A_P=5000$ ft² with x_2^f as parameter.

AEROBIC FERMENTATION OF PAUNCH LIQUOR

Mark D. Young
Department of Chemical Engineering
University of Nebraska-Lincoln
Lincoln, Nebraska 68508

The 1970 value of shipments of fresh red meats in the United States was twenty-two billion dollars. The packing industry which supplied these meats is the second largest industrial polluter in terms of BOD output per year. Data obtained from packing plants indicate that paunch liquor accounts for 15% of the effluent BOD, but comprises only 0.2% of the total plant effluent volume. This project, therefore, attempted to develop a process to convert paunch waste into an economically attractive byproduct.

Since the paunch of the cow is an anaerobic fermentation vessel designed for the degradation of cellulose, it is buffered and conditioned to produce an environment favorable for microbial activity. We proposed that it would provide a suitable medium for microbial activity under aerobic conditions which would decrease BOD while producing single cell protein.

The material which provided the medium for the growth of the organisms was collected from the paunches of seventeen heifers during the course of one day's killing operation at a local packing plant. To provide a liquid medium for the collection of data, the material was diluted with half its volume of water and pressed. Significant data on the samples is presented in Table 1.

Microorganisms which were to be candidates for the process were isolated from fresh paunch contents under aerobic conditions at 35°C. An interesting growth characteristic which accompanied each organism which grew well was its ability to increase the pH of the medium.

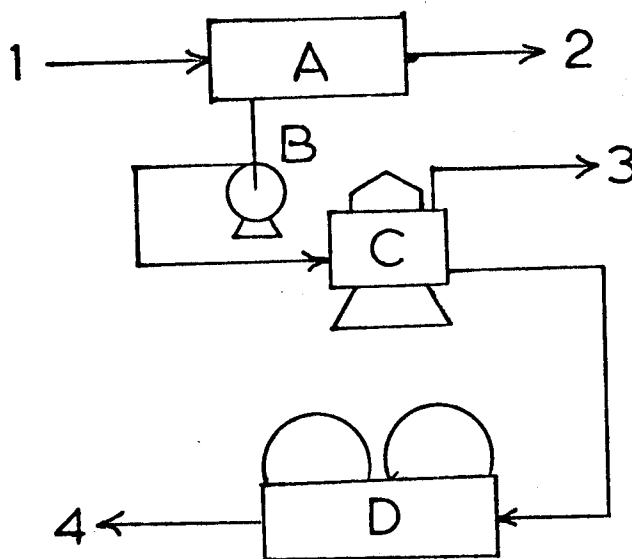
Using data obtained from the organisms and the medium, two processes were designed and cost analyses were performed. These two processes were termed Design A and Design B and their flow diagrams appear in Figures 1 and 2. Relevant economic data appear in Tables 2 and 3 for various plant capacities. Plant cost was depreciated over a 10-year period.

Comparing these methods with other processes presently in use, it is recommended that further work be done on Design A since it appears to be nearly comparable to present methods; however, under current economic conditions, Design B is unfeasible.

Acknowledgement

Support for this project was provided by the National Science Foundation under its Student-Originated Studies program.

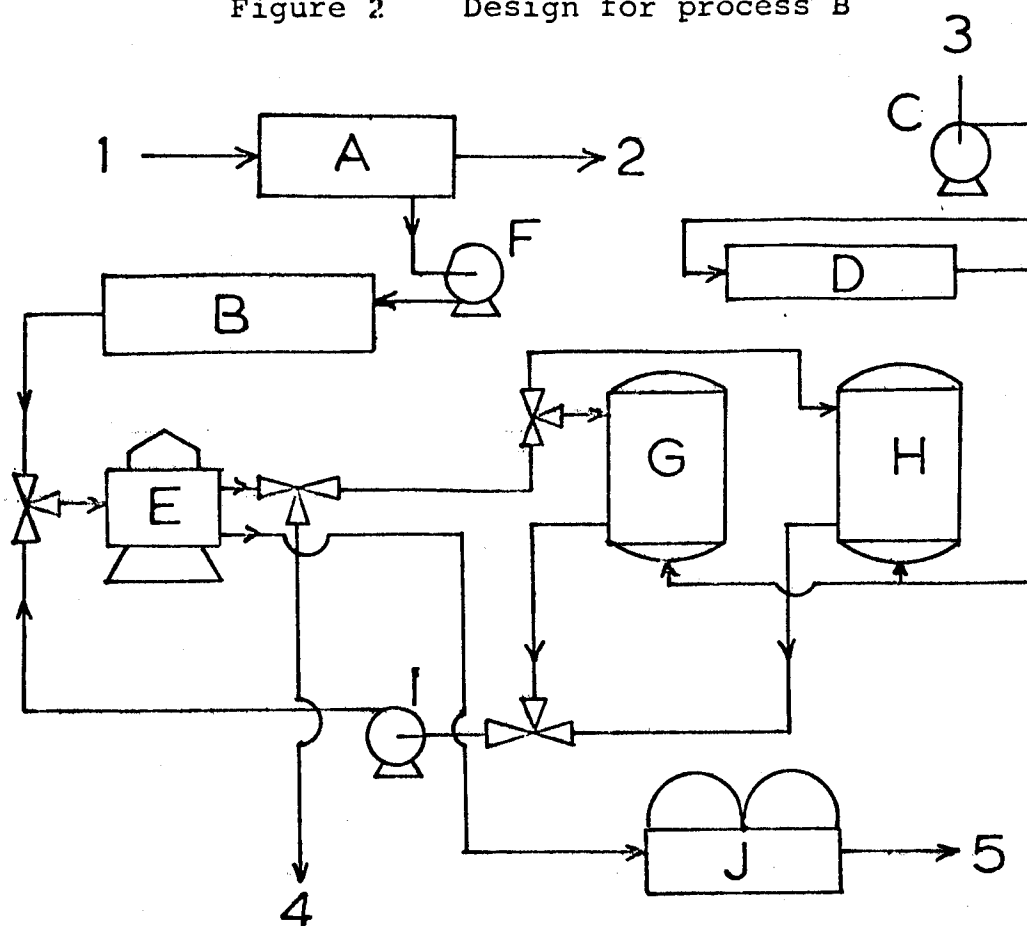
Figure 1 Design for process A



Key

A	Hydraulic press
B	Pump
C	Centrifuge
D	Drum dryer
1	Paunch contents
2	Pressed manure
3	Supernatant 16g/liter COD
4	Dried residue 40% protein

Figure 2 Design for process B



Key

A	Hydraulic press
B	Sterilization
C	Compressor pump
D	Filter
E	Centrifuge
F	Pump
G	Fermenter #1
H	Fermenter #2
I	Pump
J	Drum dryer
1	Paunch contents
2	Pressed manure
3	Air
4	Supernatant from fermentation 7 to 11 g/liter COD
5	Products from liquor residue and fermentation

Table 1

	Total Contents	Unautoclaved Extract	Autoclaved Extract	Autoclaved Centrifuged			
				7000 G		13,200 G	
				Supernatent	PPT.	Supernatent	PPT.
Total Solids	22 g/100 g	32.7 g/l	26.5 g/l	+		+	8.32 g/100g
Protein	2.49 g/100 g	11.2 g/l	8.6 g/l	4.6 g/l	2.43 $\frac{g}{100 g}$	4.33 g/l	2.7 g/100g
Red Sugar	*	.258 g/l	*	.44 g/l	*	.22 g/l	*
Cellulose	.182 g/g	+	1.01 g/l	+	+	+	.54 g/100g
COD	.266 g/g	42.2 g/l	34.2 g/l	+	+	10.71 g/l	14.7 g/100g
pH	+	5.5	5.4	5.5	+	5.5	+
Fats & Grease	*	+	2.4 g/l	+	*	+	*
Water	78% g/g	97%	97%	~100%	+	~100%	72%

* Experimental methods found not feasible

+ Test not performed